Journal of Pharmaceutical Innovation (2026) 21:248
https://doi.org/10.1007/s12247-026-10526-w

RESEARCH

Soaking-Loaded Diclofenac Sodium Buccal Films Fabricated by FDM 3D Printing

Özlem Kral[1] · Aysel Yılmaz[2]

Received: 16 January 2026 / Accepted: 19 February 2026
© The Author(s) 2026

Abstract

Intraoral drug delivery systems offer a promising alternative to conventional oral dosage forms by enabling direct systemic absorption and bypassing first-pass metabolism. In this study, diclofenac sodium (DS)-loaded intraoral films were fabricated using fused deposition modeling (FDM) 3D printing combined with a post-printing soaking-loading technique. The effects of soaking time, film pattern, and drug amount on drug loading capacity and in vitro membrane-controlled diffusion were systematically investigated. The physicochemical properties and content homogeneity of the films were evaluated, while drug-polymer compatibility was assessed using FTIR. In vitro membrane-controlled diffusion studies revealed controlled drug diffusion from all film formulations and demonstrated a significant influence of film pattern on release kinetics. After an 8-hour diffusion period, formulations F4 and F6 exhibited drug diffusion rates of 41.3% and 52.7%, respectively, whereas the DS solution showed a markedly higher diffusion rate of 78.1%. Films fabricated with a striped infill pattern displayed enhanced drug diffusion compared to flat-patterned films, which was attributed to increased surface area and the formation of microchannels within the polymer matrix that facilitated solvent penetration. Importantly, the soaking-loading approach enabled efficient drug incorporation without compromising the structural integrity of the printed films. To the best of our knowledge, this study is the first to demonstrate the combined effect of post-printing soaking-loading-based drug incorporation and film pattern design on drug diffusion behavior in FDM 3D-printed intraoral films. Overall, this strategy provides an innovative, non-invasive, and customizable platform for the development of personalized intraoral drug delivery systems.

Keywords Diclofenac sodium · Soaking method · Fused deposition modeling · 3D printing · Buccal films

Introduction

Buccal administration, once limited to local effects, is now being researched for the transport of various active substances, including small molecule drugs, peptides, and macromolecules, for both local and systemic therapies. Oral mucosal administration stands out as an effective alternative to conventional oral administration, especially in cases where a rapid onset of action is desired. Due to the extensive vascularization and comparatively low enzymatic activity of the oral mucosa, active compounds can swiftly and directly enter systemic circulation, thereby largely circumventing hepatic first-pass metabolism. These attributes render it an appropriate route of administration for active compounds with significant hepatic clearance or those that experience degradation in the gastrointestinal tract. Recent in vitro, ex vivo, and in vivo studies on buccal film systems have further demonstrated that transmucosal delivery can significantly enhance systemic bioavailability compared to conventional oral administration, supporting the clinical relevance of this route. Furthermore, its non-invasive nature, improved patient compliance, suitability for patients with swallowing difficulties, and the ease of terminating treatment when necessary are among the advantages of buccal administration [1–6].

✉ Özlem Kral
oculcu@agri.edu.tr

Aysel Yılmaz
aysel.yilmaz@lokmanhekim.edu.tr

[1] Faculty of Pharmacy, Department of Pharmaceutical Technology, Ağrı İbrahim Çeçen University, Ağrı 04100, Turkey

[2] Faculty of Pharmacy, Department of Pharmaceutical Technology, Lokman Hekim University, Ankara, Turkey

Published online: 04 March 2026

Mucoadhesive buccal films for buccal applications have a wide range of uses, particularly in pediatric and geriatric patients, as well as in specific patient populations for pain and inflammation control, cardiovascular diseases, neurological disorders, infections, hormonal therapies, and systemic treatments requiring rapid action in emergency situations [3, 7]. Dissolving or biodegradable buccal films can be produced using traditional methods such as solvent casting, as well as manufacturing methods based on three-dimensional (3D) printing technologies. The solvent casting method, although widely employed in research, has notable drawbacks, including the necessity for substantial solvent quantities and challenges in scaling up for commercial production. Moreover, challenges such as air entrapment during solvent extraction, the potential for solvent residues in the final product, and batch-to-batch variability are limitations of this approach. 3D printing technologies address numerous formulation-related challenges by facilitating the optimization of essential formulation and printing parameters, as well as delineating the printable design space [3, 8]. The applicability of different 3D printing techniques for buccal film production has been demonstrated in the literature. Films containing different active ingredients such as estradiol, propranolol hydrochloride, acetaminophen, and ketoprofen have been developed using methods such as pressure-assisted microsyringe (PAM), semi-solid extrusion, and fused deposition modeling (FDM). The effects of printing parameters, film geometry, and polymer composition on mechanical properties, mucoadhesive behavior, and drug release were evaluated for these developed films [9–12]. In the FDM method, films are obtained by manually producing filaments, mostly using hot melt extrusion (HME) [8, 13], and this study evaluates the production of buccal films using commercially available Polyvinyl alcohol (PVA) filaments.

PVA is a water-soluble polymer that does not produce toxic or harmful products when dissolved. It is commercially available in filament form for FDM printing and is widely used due to its biocompatibility, biodegradability, and compatibility with pharmaceutical applications [14, 15]. Given these properties, PVA forms a suitable polymeric matrix for the delivery of active substances. Among these agents, diclofenac sodium (DS), a nonsteroidal anti-inflammatory drug (NSAID), although its gastrointestinal side effects such as gastric ulcers are tolerable with conventional oral administration, can be considered a suitable candidate for buccal drug delivery systems due to its significant first-pass metabolism in the liver [16–18]. Conventional oral DS therapy typically involves doses ranging from approximately 25–50 mg per administration, depending on the indication and formulation. In contrast, lower drug amounts may be advantageous for localized or controlled delivery approaches via the buccal route and reduced systemic exposure are often desired. Therefore, investigating low-dose loading strategies in buccal films may represent a rational approach for controlled drug administration [19].

In FDM-based 3D printing technology, the active ingredient is usually added to the filaments used as feed material during the HME stage; however, there are also alternative methods where the active ingredient is added after filament production or subsequently to commercially available filaments [20]. In the soaking method, one of these techniques, the filament is immersed in an active ingredient solution for extended periods (hours–days), then dried until it reaches a constant weight and stored under suitable conditions before printing. During this process, the active ingredient is loaded onto the filament via diffusion, and the impregnation stage can negatively affect the surface properties and mechanical integrity of the filament, resulting in filaments unsuitable for printing [21]. Therefore, to overcome these disadvantages, in this study, the active ingredient was loaded not onto the filament, but onto the material obtained after printing using the post-printing soaking method.

On the other hand, while drug-loaded filaments produced via HME can indeed offer precise dose control through design-based approaches, they also require re-optimization of filament composition and printing conditions for each formulation change. In contrast, the post-printing soaking strategy adopted here enables dose flexibility and structural customization independently, which is particularly advantageous for personalized intraoral drug delivery systems. Although soaking introduces an additional processing step, this is offset by its methodological simplicity, adaptability, and patient-centric dosage form development.

The aim of this study is to produce PVA-based buccal films using FDM-based 3D printing technology, to load DS onto these films by post-printing soaking method, and to evaluate the potential of the resulting systems in buccal drug delivery. To our knowledge, this study is the first to comprehensively evaluate the physicochemical properties, drug content, structural characterization, and release kinetics of DS-loaded FDM-printed PVA-based buccal films and to demonstrate the combined effect of post-printing soaking-based drug incorporation and film pattern design on drug diffusion behavior.

Material Method

Materials

Polyvinyl alcohol (PVA) filament (INNOVATEFIL® PVA ULTRA, Smart Materials 3D, Spain; 1.75 mm diameter; 750 g; EAN: 8434000088713) was used as the base polymer

for film fabrication. According to the supplier's technical data sheet, the filament is water-soluble and printable at 200–240 °C, with a density of approximately 1.21 g/cm³. PVA filament was purchased from 3D Grande Technology AŞ (Türkiye). The filament was used as received. Cellulose membrane (Dialysis Tubing, molecular weight cut-off 12000–14000) was purchased from Sigma-Aldrich (USA). Diclofenac sodium (DS) was donated by Deva Holding A.Ş. (Türkiye). All other chemicals and reagents used were of pharmaceutical and analytical grade.

Film Production Using FDM 3D Printing Technology

Commercial PVA filament was loaded onto an FDM 3D printer (Anycubic 4Max Pro 2.0, China). 3D models of films were created using TinkerCad software (Autodesk Inc., USA) in two different patterns (Fig. 1) and saved in '.stl' format. The STL files were then converted to '.gcode' format using UltiMaker Cura® software (Netherlands), enabling the printer to process the files [22]. The films were produced using a 0.4 mm nozzle and with a layer height set at 0.2 mm. The extrusion temperature was maintained at 210 °C, and the build plate temperature was set to 65°C. The printing speed was fixed at 40 mm/s. An infill density of 80% was selected to balance structural integrity and internal porosity. Cooling was applied using the printer's standard fan settings. All parameters were kept constant throughout the fabrication process to ensure reproducibility.

Table 1 Process parameters for active pharmaceutical ingredient loading into 3D films

Formulation Code	Pattern	Loading Time (min)	DS solution (mg)
F1	flat	15	100
F2	flat	15	200
F3	flat	30	100
F4	flat	30	200
F5	striped	15	100
F6	striped	15	200
F7	striped	30	100
F8	striped	30	200

Diclofenac Sodium Loading of 3D Films

The post-printing soaking-loading process was conducted at 25 ± 2 °C (room temperature) under ambient laboratory conditions. This temperature was selected to ensure stable diffusion-driven drug uptake without accelerating solvent evaporation. Each film, printed at 20 × 20 mm, was individually and completely immersed in 10 mL of a water: ethanol (50:50) mixture containing DS and the containers were tightly capped [23]. Studies were conducted in solutions containing different amounts of DS (100 mg and 200 mg) for different dwell times (15 min and 30 min), as shown in Table 1. The effects of drug amount, dwell time, and pattern differences on drug loading efficiency were investigated. For each formulation, three films were prepared independently, and all experiments were performed in triplicate to ensure reproducibility.

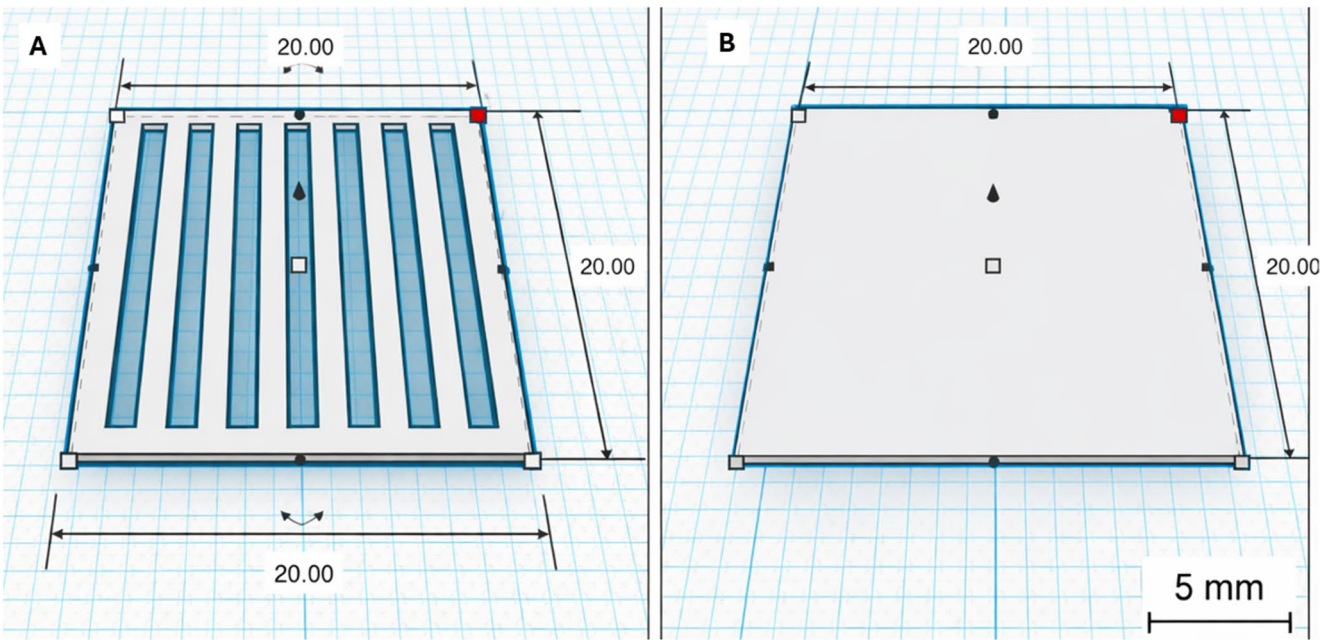

Fig. 1 CAD models of buccal films designed using Tinkercad software, illustrating the two different infill patterns employed in this study: (**A**) striped pattern and (**B**) flat pattern

Characterization Studies of Diclofenac Sodium Buccal Films

Physical Examination

Films immersed in an ethanol: water mixture were visually inspected after drying. The integrity, flexibility, and brittleness of the film structure were physically examined.

Weight and Thickness Analysis

The side length and thickness of the films were determined using a digital micrometer and the weight homogeneity was evaluated with a precision balance [22]. All experiments were performed in triplicate to ensure reproducibility.

Drug Content and Drug Loading Efficiency Analysis

The films were removed from the DS solution at the end of the soaking period and dried at room temperature until they reached constant weight. After drying, the films were individually dissolved in 50 mL of pH 6.8 phosphate buffer at 37 °C by stirring. Samples were filtered using membrane syringe filters and then analyzed with a UV spectrophotometer at 287 nm, and the amount of DS loaded per film was determined. The percentage of DS content and drug loading efficiency was calculated according to Eq. 1 [23] and Eq. 2 [24].

$$Drug\ content\ (w/w) = (Mass\ of\ drug\ in\ film/Mass\ of\ film) \quad (1)$$

$$Drug\ loading\ efficiency\ (\%) = (Actual\ drug\ content/Theoretical\ drug\ loading) \times 100 \quad (2)$$

For content homogeneity testing, three 10 × 10 mm samples were taken from different regions each 20 × 20 mm film. The samples were dissolved in phosphate buffer (pH 6.8), and drug content was quantified spectrophotometrically. Homogeneity was evaluated by comparing the drug content among samples ($n = 3$).

Fourier Transform Infrared Spectroscopy (FTIR)

In order to determine the functional groups of DS, blank PVA films, and DS-loaded films and to investigate the possible interactions between them, FTIR scanning of single and 1:1 physical mixtures was performed over the range of 4000–600 cm^{-1} wavenumber. Each spectrum was collected with a resolution of 4 cm^{-1} by averaging 32 scans per sample. The samples were analyzed in solid form without dilution and were placed directly onto the ATR crystal under uniform pressure to ensure consistent contact [25].

In Vitro Membrane-Controlled Diffusion and Kinetic Studies

The in vitro diffusion of DS from 3D films was assessed utilizing Franz diffusion cells equipped with a cellulose membrane (Dialysis Tubing, molecular weight cut-off 12000–14000, Sigma-Aldrich, USA). Films measuring 10 × 10 mm were positioned in the donor chamber, while the acceptor phase was filled with 2.5 mL of pH 6.8 phosphate buffer. After placing the film in the donor compartment, approximately 100 µL of phosphate buffer (pH 6.8) was added to ensure initial hydration and uniform membrane contact prior to the start of the experiment. The receptor phase was continuously stirred at 250 rpm using a magnetic stirrer throughout the in vitro membrane-controlled diffusion experiments to ensure uniform drug distribution. Samples were extracted from the acceptor phase at designated time intervals (10, 20, 30, 60, 90, 120, 180, 240, 360 and 480 min), and an equivalent volume of new buffer solution was promptly added to maintain sink conditions [26, 27]. UV spectrophotometry was used to determine the amount of DS. Experiments were conducted in triplicate ($n = 3$).

A DS solution was prepared as a reference for comparison with the film formulations during the in vitro membrane-controlled diffusion study. Briefly, 100 mg of DS was dissolved in 10 mL of distilled water under magnetic stirring until complete dissolution was achieved.

The diffusion data were fitted using DDSolver. Zero-order, first-order, Higuchi, Hixson-Crowell, and Korsmeyer-Peppas models were evaluated to determine the best fit for the drug release kinetics (Table 2) [28].

Statistical Analysis

The data obtained from the experiments were statistically analyzed. The Student's t-test were employed. Graphs were produced with GraphPad Prism® 5.0 software for statistical analysis. DDSolver was used for in vitro release kinetic

Table 2 Kinetic model equations

Model	Equation
Zero Order	$F = k_0 t$
First Order	$F = 100\ [1\text{-}Exp(-k_1\ t)]$
Higuchi	$F = k_H\ t^{0.5}$
Hixson-Crowell	$F = 100\ [1\text{-}(1\text{-}k_{HC}\ t)^3]$
Korsmeyer-Peppas	$F = k_{KP}\ t^n$

*F = drug released (%); t = time (hours)

studies. All experiments were performed in triplicate to ensure reproducibility.

Result and Discussion

Physical Characteristics

Following the soaking process in an ethanol: water mixture, it was observed that all films retained their primary structure and did not undergo deformation (Fig. 2). Throughout the experimental procedures, including soaking, drying, and in vitro membrane-controlled diffusion testing, the films maintained their structural integrity and flexibility without observable cracking or fragmentation. This suggests that the FDM-printed films possessed sufficient mechanical robustness for laboratory handling and preliminary buccal application studies.

Since ethanol alone is not a solvent for PVA [29], the film matrix remained undissolved; however, the penetration of the solvent between the polymer chains resulted in increased film flexibility. With increasing soaking time, a limited disruption in structural integrity was observed due to partial swelling of the polymer matrix, resulting in softer, more flexible films. Molecular dynamics simulation studies have revealed the swelling behavior of PVA in ethanol solutions containing different water ratios (15%, 30%, and 45% w/w). These studies showed that as PVA swells, the free volume changes due to a reduction in crystallinity, and the mobility of the polymer chains increases significantly [30]. These findings suggest that ethanol-water mixtures can create a plasticizer-like effect by increasing polymer chain mobility within the PVA matrix.

Weight and Thickness Analysis

The geometry of the films did not vary according to the CAD design, and the average film thickness was measured as 0.4 mm and the side length as 20 mm. Prior to drug loading, the film weights of the F1-F4 formulations ranged from 235.2 ± 0.32 to 235.8 ± 0.35 mg, while those of the F5-F8 formulations ranged from 180.2 ± 0.18 to 180.6 ± 0.19 mg. After drug loading, the film weights showed a narrow range: 234.2 ± 5.36 to 245.9 ± 7.22 mg for the F1-F4 formulations and 176.2 ± 6.12 to 189.4 ± 8.46 mg for the F5-F8 formulations (Fig. 3). This suggest that the drug loading process did not cause noticeable variation in film weights (unpaired Student's t-tests, $p > 0.05$). On the other hand, when the infill pattern is striped, the voids within the film increase; therefore, films printed with a higher infill pattern are expected to exhibit greater weight. As infill density increases, the amount of material extruded during printing increases, and consequently, the part weight increases linearly [31].

Drug Content and Drug Loading Efficiency Analysis

DS was loaded onto buccal films by the post printing-soaking method. In the soaking method, the drug is dispersed into the polymer matrix via passive diffusion and becomes trapped within the matrix after the drying stage [29].

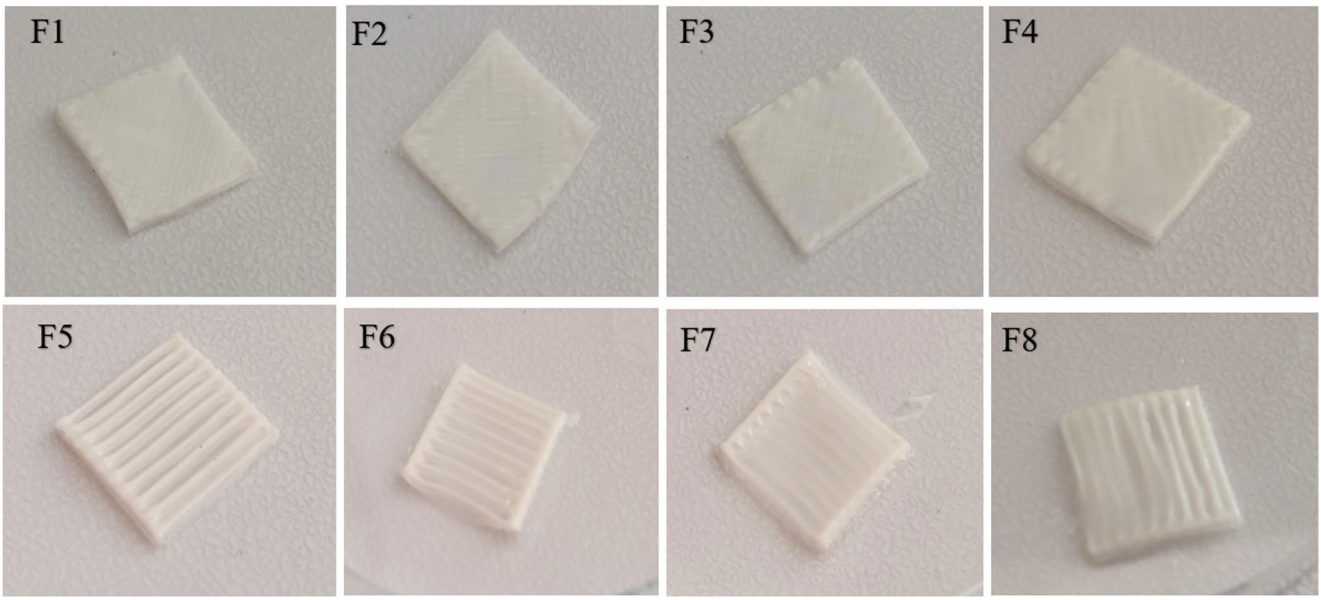

Fig. 2 Photographs of DS-loaded PVA-based buccal films fabricated by FDM 3D printing, illustrating their visual appearance with different infill patterns. Films F1-F4 represent flat-pattern designs, while films F5-F8 correspond to striped-pattern designs, highlighting the influence of internal structure on the final film architecture ($n = 3$)

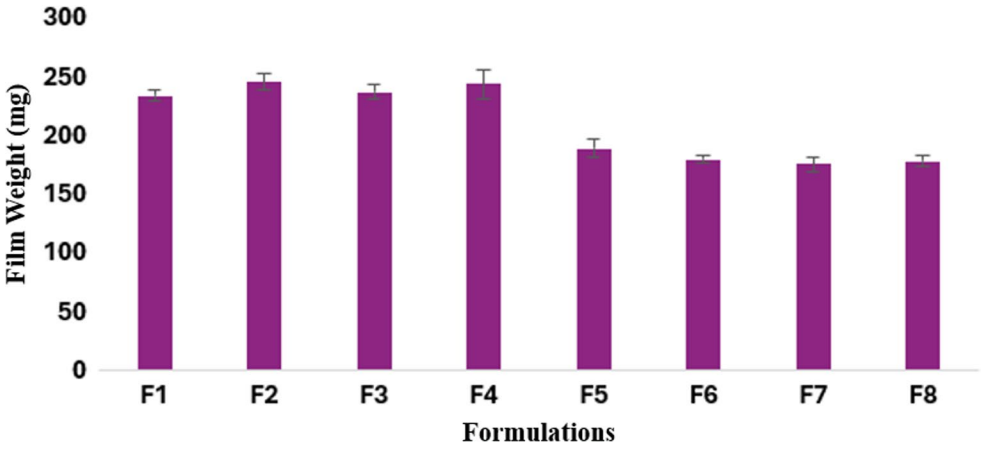

Fig. 3 Weight variation of DS-loaded PVA-based buccal films fabricated by FDM 3D printing. Films F1-F4 correspond to flat infill patterns, whereas films F5-F8 represent striped infill patterns. Data are presented as mean ± SD, demonstrating the effect of infill pattern on film weight following post-printing soaking ($n = 3$)

Soaking is a widely used technique in the literature for loading active substances onto pre-fabricated filaments. Goyanes et al. performed drug loading on PVA filaments using an ethanolic solution containing 2% (w/v) fluorescein; for this purpose, the filaments were kept in the active substance solution for 24 h under magnetic stirring. After the loading process, the filaments were dried, and the final drug loading was reported as 0.29 ± 0.01% (w/w) in the filaments. Subsequently, tablets with different infill density were produced using 3D printing technology [29]. Tagami et al. used the soaking method to load curcumin onto PVA filaments; they evaluated the effects of different types of organic solvents (isopropanol, methanol, acetone, and ethanol), temperature (25 and 80 °C), and drug concentration (2–333 mg/mL) on drug loading efficiency. In the study, approximately 5% curcumin was loaded onto the filaments, and tablets were produced using 3D printing technology with the obtained filaments [32]. Ibrahim et al. used the soaking method to load metformin HCl dissolved in an ethanol-water (9:1) mixture onto PVA filaments. It was reported that the drug loading increased in the first few days depending on the soaking time, but reached equilibrium in the following days, and that prolonged soaking had a limited effect on the loading efficiency [23]. In this study, active ingredient loading was not performed at the filament stage; instead, the resulting films were loaded using the post-printing soaking method. One of the significant advantages of this approach is that the filament diameter and geometric integrity are preserved because the filament is not directly wetted. Since diameter changes, surface deformations, and potential deteriorations in mechanical properties that may occur when the filament is wetted can negatively affect print quality and repeatability, the post-printing soaking method prevents these disadvantages and ensures the stability of the printing process.

The drug content was determined to be in the range of 9.90 ± 2.10–18.7 ± 3.12 µg/mg in formulations F1-F4 and 12.3 ± 2.15–20.2 ± 2.51 µg/mg in formulations F5-F8 (Fig. 4). In addition, Table 3 presents the drug loading efficiency (%) values of the film formulations. Drug loading results show that the post-printing wetting approach ensures reproducible incorporation of diclofenac sodium into PVA films, with loading efficiencies ranging from 1.53 ± 0.09% to 2.39 ± 0.08%. These values fall within the ranges reported in the literature [29, 32] and demonstrate that the applied loading method offers a significant advantage when considering the preservation of structural integrity. Statistical analysis was performed using unpaired Student's *t*-tests. No statistically significant differences were observed between F1 and F3 in terms of

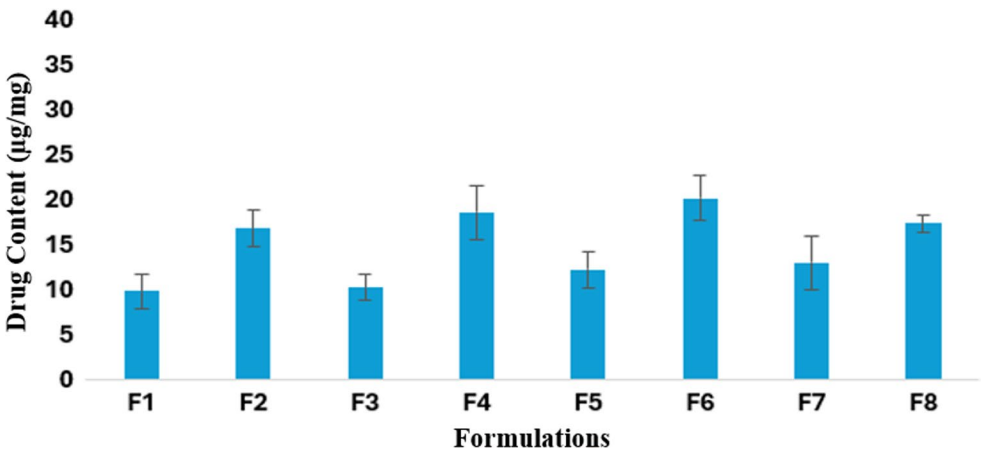

Fig. 4 DS loading capacity of PVA-based buccal films fabricated by FDM 3D printing and loaded via post-printing soaking. Films F1-F4 correspond to flat infill patterns, while films F5-F8 represent striped infill patterns. Results are expressed as micrograms of DS per milligram of film (µg/mg) and presented as mean ± SD, demonstrating the effect of infill pattern on drug loading capacity ($n = 3$)

Table 3 Drug loading efficiency (%) values of the film formulations ($n=3$)

Formulations	Drug loading efficiency (%)
F1	2.39 ± 0.08
F2	1.91 ± 0.07
F3	2.38 ± 0.06
F4	2.00 ± 0.13
F5	2.17 ± 0.02
F6	1.53 ± 0.09
F7	1.79 ± 0.03
F8	1.60 ± 0.08

drug content and loading efficiency ($p > 0.05$). Similarly, comparison between F2 and F4 did not reveal a statistically significant difference ($p > 0.05$). On the other hand, statistically significant differences exist between F5 and F6, as well as between F1 and F2 ($p < 0.05$). These findings indicate that, for both pattern designs, increasing the amount of active substance during the 15-minute soaking period resulted in significant increases in drug content and drug loading efficiency. When formulations with different pattern designs were compared, statistically significant differences in drug loading efficiency were observed between F1 and F5, F2 and F6, F3 and F7, and F4 and F8 ($p < 0.05$). However, no statistically significant differences were detected in terms of drug content ($p > 0.05$).

When the drug loading results were evaluated, it was observed that varying the loading time between 15 and 30 min did not have a significant effect on the amount of DS loaded per film. In contrast, increasing the theoretical drug amount and changing the film pattern significantly affected

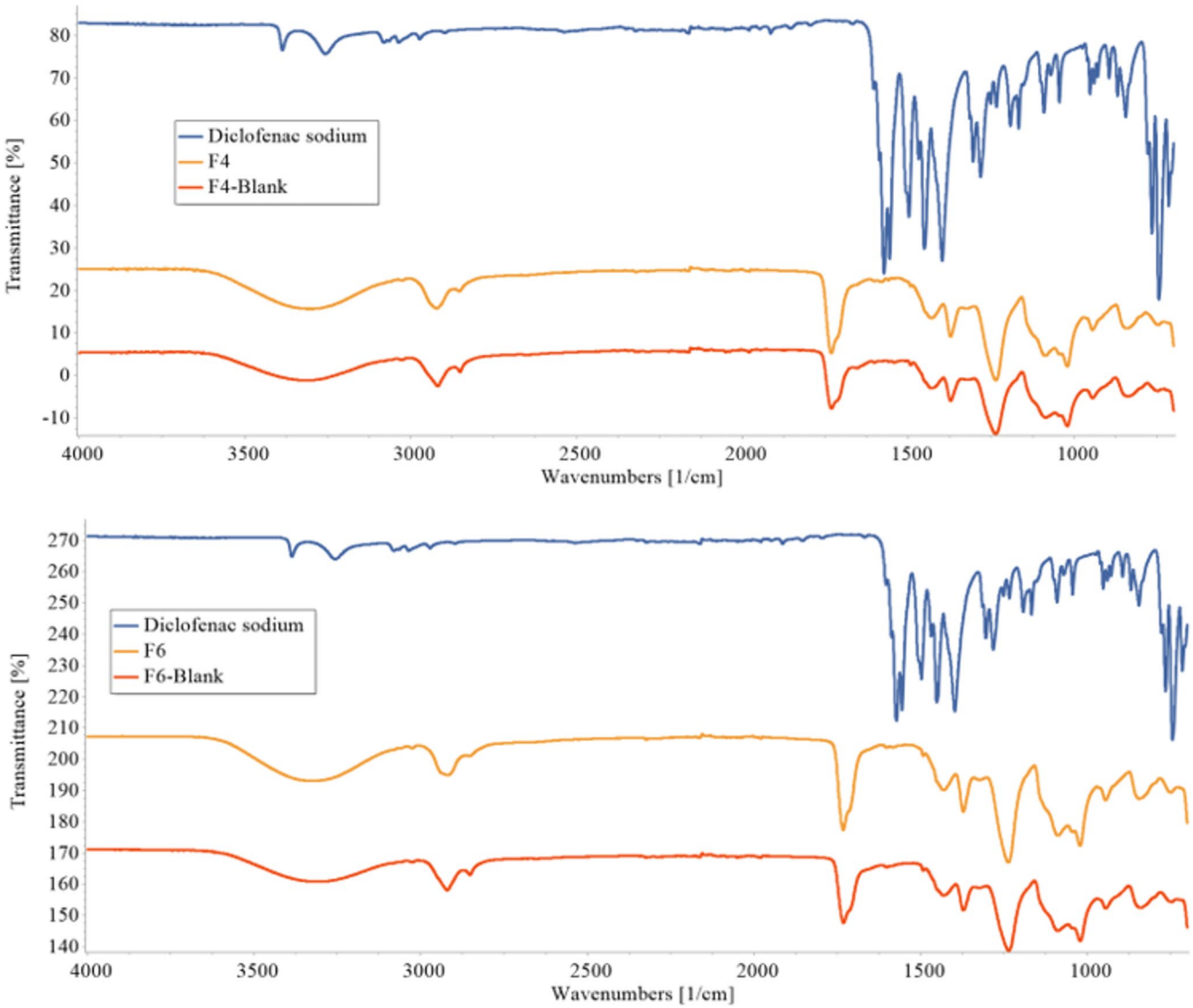

Fig. 5 FTIR spectra of pure DS, DS-loaded, and blank PVA-based buccal films fabricated by FDM 3D printing. Representative formulations F4 and F6 are presented to assess drug-polymer compatibility after post-printing drug loading. The spectra indicate no apparent chemical interaction between DS and the polymer matrix

drug loading. Specifically, the F6 formulation with a striped pattern and a theoretical drug content of 200 mg showed the highest drug loading value. While the limited effect of loading time can be explained by the rapid equilibrium of drug diffusion during the soaking method, the increase in surface area due to the pattern and drug amount is considered the main factors increasing drug loading.

FTIR Analysis

Figure 5 shows the FTIR spectra of DS, DS-loaded films and empty films. Characteristic peaks of DS were observed at approximately 1573 cm^{-1}, 3387 cm^{-1}, 3258 cm^{-1} and 750 cm^{-1} [33]. Specific peaks of DS, at 1573 and 750 cm^{-1}, were also observed in films loaded with DS. Possible interactions between DS and the polymer matrix may lead to slight shifts or changes in peak intensity. As the DS concentration decreased, the DS peaks' intensity in the film compositions' FTIR spectra also decreased [34, 35]. The characteristic peaks of PVA filaments were observed [36] both before and after the soaking process, indicating that the polymer backbone remained structurally intact and that no significant chemical alteration occurred during drug loading.

In Vitro Membrane-Controlled Diffusion and Kinetic Studies

In vitro membrane-controlled diffusion studies were performed on formulations F4 and F6, which had the highest drug loading and different infill patterns, and on the solution formulation of DS. After an 8-hour (480 min) diffusion period, it was determined that formulation F4 showed a drug diffusion rate of 41.3%, while formulation F6 showed a diffusion rate of 52.7% (Fig. 6). In contrast, the solution formulation exhibited a diffusion rate of 78.1% over the same period. When the infill pattern was striped, the voids within the film increase. The higher drug diffusion observed in striped patterned films compared to flat-patterned films can be attributed to the increased effective surface area and the potential formation of microchannels within the polymer matrix that facilitate solvent penetration [22]. However, this interpretation remains a hypothesis based on the observed diffusion trends, as direct structural imaging has not been performed. Various studies have reported that drug release is related to the surface area/volume ratio, and that the release rate increases significantly with an increase in this ratio. Goyanes et al. found that drug release from 3D-printed tablets in cube, pyramid, cylinder, sphere, and ring shapes depended not on surface area but on the surface area/volume ratio; this demonstrates the effect of geometric shape on drug release [37]. In a study conducted by Khaled et al. using paracetamol, it was also reported that in vitro release results were affected by the surface area/volume ratio [38]. In this study, the fact that striped patterned films showed greater active substance diffusion compared to flat patterned films due to providing a higher effective surface area at a constant volume is considered a result consistent with the findings reported in the literature. However, the Franz diffusion method is also thought to have an effect on the diffusion behavior. The fact that DS did not reach 100% permeation during the eight-hour experiment can be explained by the fact that the parameter measured in the Franz diffusion cell reflects the membrane-controlled diffusion process acting as

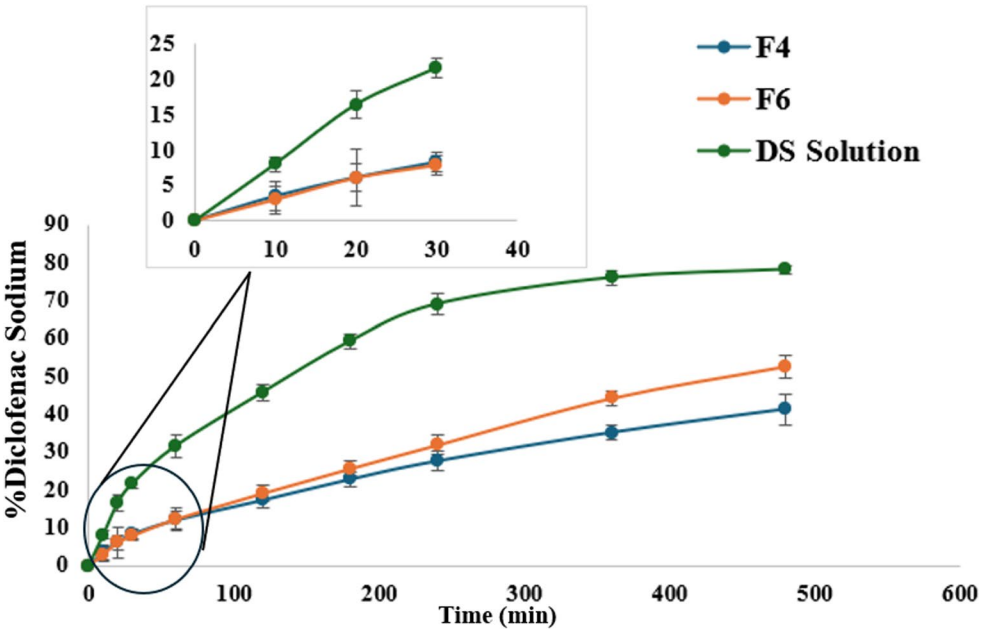

Fig. 6 In vitro membrane-controlled diffusion profiles of DS from PVA-based buccal films fabricated by FDM 3D printing ($n=3$). Representative formulations F4 (flat infill) and F6 (striped infill) are compared with a DS solution as the reference. Data are presented as mean ± SD. The inset highlights the initial diffusion phase, illustrating differences in early drug diffusion behavior among the formulations

Table 4 Models' statistical parameters for describing DS's in vitro membrane-controlled diffusion

		F4	F6	DS Solution
Zero order	**R^2_{adj}**	0.89	0.95	0.67
	AIC	54.80	51.00	80.30
	MSC	1.79	2.72	0.65
First order	**R^2_{adj}**	0.94	0.99	0.93
	AIC	48.50	37.60	64.50
	MSC	2.42	4.06	2.22
Higuchi	**R^2_{adj}**	0.98	0.95	**0.97**
	AIC	34.50	51.00	**54.90**
	MSC	3.83	2.72	**3.19**
Hixson-Crowell	**R^2_{adj}**	0.92	0.98	0.88
	AIC	50.70	42.30	69.60
	MSC	2.21	3.59	1.72
Korsmeyer -Peppas	**R^2_{adj}**	**0.99**	**0.99**	0.94
	AIC	**8.74**	**15.90**	63.80
	MSC	**6.40**	**6.23**	2.29
	n	**0.59**	**0.66**	0.57

*R^2_{adj} adjusted coefficient of determination, *MSC* Model Selection Criterion, *AIC* Akaike Information Criterion (AIC), *n* diffusion exponents,indicative of the drug release mechanism

a barrier rather than actual release [39]. Also, it has been reported that drug release rates tend to decrease for active substances with higher molecular weight [40].

Release kinetics were evaluated using five commonly used mathematical models, and both formulations F4 and F6 were found to show the best fit to the Korsmeyer-Peppas model. In contrast, the diffusion profile of DS in solution was observed to be consistent with the Higuchi model (Table 4). The release exponent (n) values calculated according to the Korsmeyer-Peppas model were determined as 0.591 and 0.659 for formulations F4 and F6, respectively. In the literature, it is known that $n \leq 0.45$ corresponds to a Fickian diffusion mechanism, values in the range of $0.45 < n < 0.89$ correspond to non-Fickian (abnormal) transport, $n = 0.89$ corresponds to state II transport, and $n > 0.89$ corresponds to super-state II transport [41]. Accordingly, the results obtained show that in both film formulations, the release behavior follows a non-Fickian (anomalous) transport mechanism involving drug diffusion occurring along with swelling and erosion of the polymer matrix. The most suitable release model for the solution form of DS was determined to be the Higuchi model; the high correlation (R^2) values obtained in this model revealed that the drug release mechanism is primarily diffusion-controlled [42].

DDSolver provides several statistical criteria for evaluating dissolution models. Among these, R^2_{adj}, AIC, and MSC are commonly used for selecting the most appropriate model. A higher R^2_{adj} value, lower AIC, and higher MSC indicate a better fit of the mathematical model to the experimental data [43].

Conclusion

In this study, DS-loaded intraoral films were successfully fabricated using FDM 3D printing combined with a post-printing soaking-loading method. DS was deliberately incorporated after film fabrication and therefore was not exposed to filament production or FDM processing conditions. This approach allowed the printing process and the drug incorporation step to be decoupled, enabling the same printed film architecture to be used as a flexible platform for different drug amounts without modifying filament composition or printing parameters. The results demonstrated that the soaking-loading method is an effective strategy for incorporating drug into 3D-printed polymeric films without adversely affecting their structural integrity or physicochemical properties. Controlled drug diffusion profiles were achieved, confirming the suitability of the developed films for intraoral drug delivery applications. Importantly, the study revealed that both soaking parameters and film design play critical roles in determining drug loading capacity and release behavior. In particular, modification of the infill pattern significantly influenced release kinetics, with striped-patterned films exhibiting enhanced drug diffusion due to increased surface area and the formation of potential microchannels within the polymer matrix. These findings highlight the potential of 3D printing-based structural customization as a powerful tool for tailoring drug release profiles without altering formulation composition.

Author Contributions Ö.K and A.Y. carried out the lab works and wrote the first draft. Ö.K supervised the works and methodology. All authors have read and approved the final manuscript.

Funding Open access funding provided by the Scientific and Technological Research Council of Türkiye (TÜBİTAK).

Data Availability All data are in the manuscript and/or supporting information files.

Declarations

Competing interests The authors declare no competing interests.

Open Access This article is licensed under a Creative Commons Attribution 4.0 International License, which permits use, sharing, adaptation, distribution and reproduction in any medium or format, as long as you give appropriate credit to the original author(s) and the source, provide a link to the Creative Commons licence, and indicate if changes were made. The images or other third party material in this article are included in the article's Creative Commons licence, unless indicated otherwise in a credit line to the material. If material is not included in the article's Creative Commons licence and your intended use is not permitted by statutory regulation or exceeds the permitted use, you will need to obtain permission directly from the copyright holder. To view a copy of this licence, visit http://creativecommons.org/licenses/by/4.0/.

References

1. Bahraminejad S, Almoazen H. Sublingual and buccal delivery: a historical and scientific prescriptive. Pharmaceutics. 2025;17:1073. https://doi.org/10.3390/pharmaceutics17081073.
2. Hua S. Advances in nanoparticulate drug delivery approaches for sublingual and buccal administration. Front Pharmacol Front Media SA. 2019;10:1328. https://doi.org/10.3389/fphar.2019.01328.
3. Jacob S, Nair AB, Boddu SHS, Gorain B, Sreeharsha N, Shah J. An updated overview of the emerging role of patch and film-based buccal delivery systems. Pharmaceutics. 2021;13:1206. https://doi.org/10.3390/pharmaceutics13081206.
4. Wang S, Jiang L, Meng S, Liu C, Wang H, Gao Z, et al. Hollow mesoporous silica nanoparticles-loaded ion-crosslinked bilayer films with excellent mechanical properties and high bioavailability for buccal delivery. Int J Pharm. 2022;624:122056. https://doi.org/10.1016/j.ijpharm.2022.122056.
5. Wang S, Liu L, Meng S, Wang Y, Liu D, Gao Z, et al. A method for evaluating drug penetration and absorption through isolated buccal mucosa with highly accuracy and reproducibility. Drug Deliv Transl Res. 2022;12:2875–92. https://doi.org/10.1007/s13346-022-01151-4.
6. Wang S, Gao Z, Liu L, Li M, Zuo A, Guo J, et al. Preparation, in vitro and in vivo evaluation of chitosan-sodium alginate-ethyl cellulose polyelectrolyte film as a novel buccal mucosal delivery vehicle. Eur J Pharm Sci. 2022. https://doi.org/10.1016/j.ejps.2021.106085.
7. Shipp L, Liu F, Kerai-Varsani L, Okwuosa TC. Buccal films: a review of therapeutic opportunities, formulations & relevant evaluation approaches. J Controlled Release Elsevier. 2022;352:1071–92. https://doi.org/10.1016/j.jconrel.2022.10.058.
8. Elkanayati RM, Chambliss WG, Omari S, Almutairi M, Repka MA, Ashour EA. Mucoadhesive buccal films for treatment of xerostomia prepared by coupling HME and 3D printing technologies. J Drug Deliv Sci Technol. 2022;75:103660. https://doi.org/10.1016/j.jddst.2022.103660.
9. Abdella S, Afinjuomo F, Song Y, Upton R, Garg S, Elsevier B.V. 3D printed bilayer mucoadhesive buccal film of estradiol: impact of design on film properties, release kinetics and predicted in vivo performance. Int J Pharm. 2022. https://doi.org/10.1016/j.ijpharm.2022.122324.
10. Eleftheriadis GK, Monou PK, Bouropoulos N, Boetker J, Rantanen J, Jacobsen J, et al. Fabrication of mucoadhesive buccal films for local administration of ketoprofen and lidocaine hydrochloride by combining fused deposition modeling and inkjet printing. J Pharm Sci. 2020;109:2757–66. https://doi.org/10.1016/j.xphs.2020.05.022.
11. Jovanović M, Petrović M, Cvijić S, Tomić N, Stojanović D, Ibrić S, et al. 3D printed buccal films for prolonged-release of propranolol hydrochloride: development, characterization and bioavailability prediction. Pharmaceutics. 2021;13:2143. https://doi.org/10.3390/pharmaceutics13122143.
12. Zhang J, Lu A, Thakkar R, Zhang Y, Maniruzzaman M. Development and evaluation of amorphous oral thin films using solvent-free processes: comparison between 3D printing and hot-melt extrusion technologies. Pharmaceutics. 2021;13:1613. https://doi.org/10.3390/pharmaceutics13101613.
13. Chen H, Li X, Gong Y, Bu T, Wang X, Pan H. Unidirectional drug release from 3D printed personalized buccal patches using FDM technology. Int J Pharm. 2023;645:123382. https://doi.org/10.1016/j.ijpharm.2023.123382.
14. Bazhenov VE, Krutsky AA, Lyskovich AA, Rizhsky AA, Kovyshkina EP, Tselovalnik YV, et al. The utilization of Polyvinyl Alcohol (PVA) filaments for the three-dimensional printing of water-soluble patterns for investment casting. J Manuf Mater Process. 2025;9:48. https://doi.org/10.3390/jmmp9020048.
15. Bianchi M, Pegoretti A, Fredi G. An overview of poly (vinyl alcohol) and poly (vinyl pyrrolidone) in pharmaceutical additive manufacturing. J Vinyl Addit Technol. 2023;29:223–39. https://doi.org/10.1002/vnl.21982.
16. El-Samaligy MS, Yahia SA, Basalious EB. Formulation and evaluation of diclofenac sodium buccoadhesive discs. Int J Pharm. 2004;286:27–39. https://doi.org/10.1016/j.ijpharm.2004.07.033.
17. Todd PA, Sorkin EM. Diclofenac sodium: a reappraisal of its pharmacodynamic and pharmacokinetic properties, and therapeutic efficacy. Drugs. 1988;35:244–85. https://doi.org/10.2165/00003495-198835030-00004.
18. Willis JV, Kendall MJ, Flinn RM, Thornhill DP, Welling PG. The pharmacokinetics of diclofenac sodium following intravenous and oral administration. Eur J Clin Pharmacol Springer. 1979;16:405–10. https://doi.org/10.1007/BF00568201.
19. Sheoran R. Buccal drug delivery system: a review. Int J Pharm Sci Rev Res. 2018;50:40–6.
20. Ahmed Y, Mahmoud AAK, Ludasi K, Sovány T, Multidisciplinary Digital Publishing Institute (MDPI). Advances in loading techniques and quality by design for fused deposition modeling in pharmaceutical production: a systematic review. Pharmaceuticals. 2024. https://doi.org/10.3390/ph17111496.
21. Cailleaux S, Sanchez-Ballester NM, Gueche YA, Bataille B, Soulairol I. Fused deposition modeling (FDM), the new asset for the production of tailored medicines. J Control Release. 2021;330:821–41. https://doi.org/10.1016/j.jconrel.2020.10.056.
22. Yilmaz A, Mutlu-Agardan NB, Takka S. Development of immediate release tablet formulations of lornoxicam with hot melt extrusion-based three-dimensional printing technology. Drug Dev Ind Pharm Taylor Francis Ltd. 2025;51:64–76. https://doi.org/10.1080/03639045.2024.2447277.
23. Ibrahim M, Barnes M, McMillin R, Cook DW, Smith S, Halquist M, et al. 3D printing of Metformin HCl PVA tablets by fused deposition modeling: drug loading, tablet design, and dissolution studies. AAPS PharmSciTech. 2019. https://doi.org/10.1208/s12249-019-1400-5.
24. Kheawfu K, Panraksa P, Jantrawut P, MDPI. Formulation and characterization of Nicotine microemulsion-loaded fast-dissolving films for smoking cessation. Molecules. 2022. https://doi.org/10.3390/molecules27103166.
25. Kral Ö, Eralmaç A, Aydin T, John Wiley and Sons Inc. Development and characterization of a topical Herniarin ointment from Tarragon. ChemistrySelect. 2025. https://doi.org/10.1002/slct.202500651.
26. Gorle A, Patil P, Bhaskar R, Ola M. Development and evaluation of buccal film containing antihypertensive agent [Internet]. ~53~The Pharma Innovation Journal. 2015. www.thepharmajournal.com.
27. Singh S, Jain S, Muthu MS, Tiwari S, Tilak R. Preparation and evaluation of buccal bioadhesive films containing clotrimazole. AAPS PharmSciTech. 2008;9:660–7. https://doi.org/10.1208/s12249-008-9083-3.
28. Erawati E, Hamid H, Musthofa M, Fatoni R, Nurwaini S, Rahmah AU, et al. Drug release kinetics of capsule shells from seaweed carrageenan extract (*Eucheuma cottonii*) and potato starch as a gelling agent. Bull Natl Res Cent. 2023. https://doi.org/10.1186/s42269-023-01045-6.
29. Goyanes A, Buanz ABM, Basit AW, Gaisford S. Fused-filament 3D printing (3DP) for fabrication of tablets. Int J Pharm Elsevier. 2014;476:88–92. https://doi.org/10.1016/j.ijpharm.2014.09.044.
30. Zhang QG, Liu QL, Chen Y, Wu JY, Zhu AM. Microstructure dependent diffusion of water–ethanol in swollen poly (vinyl alcohol): a molecular dynamics simulation study. Chem Eng Sci Elsevier. 2009;64:334–40. https://doi.org/10.1016/j.ces.2008.10.028.

31. Derise MR, Zulkharnain A. Effect of infill pattern and density on tensile properties of 3d printed polylactic acid parts via fused deposition modeling (FDM). Int J Mech Mechatron Eng. 2020;20:56–63.
32. Tagami T, Kuwata E, Sakai N, Ozeki T. Drug incorporation into polymer filament using simple soaking method for tablet preparation using fused deposition modeling. Biol Pharm Bull Pharm Soc Japan. 2019;42:1753–60. https://doi.org/10.1248/bpb.b19-00482.
33. Liu D, Chen L, Jiang S, Zhu S, Qian Y, Wang F, et al. Formulation and characterization of hydrophilic drug diclofenac sodium-loaded solid lipid nanoparticles based on phospholipid complexes technology. J Liposome Res. 2014;24:17–26. https://doi.org/10.3109/08982104.2013.826241.
34. Kral Ö, Hennep G, Uslu EN, Yücel Ç, Springer. Formulation and cytotoxicity assessment of methylprednisolone aceponate microemulsions for topical delivery. J Pharm Innov. 2026;21:38. https://doi.org/10.1007/s12247-025-10275-2.
35. Jagdale S, Chandekar A. Optimization of chitosan and cellulose acetate phthalate controlled delivery of methylprednisolone for treatment of inflammatory bowel disease. Adv Pharm Bull Tabriz Univ Med Sci. 2017;7:203–13. https://doi.org/10.15171/apb.2017.025.
36. Bazhenov VE, Krutsky AA, Lyskovich AA, Rizhsky AA, Kovyshkina EP, Tselovalnik YV, et al. The utilization of Polyvinyl Alcohol (PVA) filaments for the three-dimensional printing of water-soluble patterns for investment casting. Journal of Manufacturing and Materials Processing. 2025. https://doi.org/10.3390/jmmp9020048.
37. Goyanes A, Martinez PR, Buanz A, Basit AW, Gaisford S. Effect of geometry on drug release from 3D printed tablets. Int J Pharm Elsevier. 2015;494:657–63. https://doi.org/10.1016/j.ijpharm.2015.04.069.
38. Khaled SA, Alexander MR, Irvine DJ, Wildman RD, Wallace MJ, Sharpe S, et al. Extrusion 3D printing of paracetamol tablets from a single formulation with tunable release profiles through control of tablet geometry Springer. AAPS PharmSciTech. 2018;19:3403–13. https://doi.org/10.1208/s12249-018-1107-z.
39. Kumar M, Sharma A, Mahmood S, Thakur A, Mirza MA, Bhatia A. Franz diffusion cell and its implication in skin permeation studies. J Dispers Sci Technol Taylor Francis. 2024;45:943–56. https://doi.org/10.1080/01932691.2023.2188923.
40. Sa'adon S, Abd Razak SI, Fakhruddin K, Elsevier. Drug-loaded poly-vinyl alcohol electrospun nanofibers for transdermal drug delivery: review on factors affecting the drug release. Procedia Comput Sci. 2019;158:436–42. https://doi.org/10.1016/j.procs.2019.09.073.
41. Đuranović M, Madžarević M, Ivković B, Ibrić S, Cvijić S, Elsevier. The evaluation of the effect of different superdisintegrants on the drug release from FDM 3D printed tablets through different applied strategies: in vitro-in silico assessment. Int J Pharm. 2021;610:121194. https://doi.org/10.1016/j.ijpharm.2021.121194.
42. Khan S, Ranjha NM. Effect of degree of cross-linking on swelling and on drug release of low viscous chitosan/poly (vinyl alcohol) hydrogels. Polym Bull. 2014;71:2133–58. https://doi.org/10.1007/s00289-014-1178-2.
43. Kral Ö, Ilbasmis-Tamer S, Han S, Tirnaksiz F, American Chemical Society. Development of dermal lidocaine nanosuspension formulation by the wet milling method using experimental design: in vitro/in vivo evaluation. ACS Omega. 2024. https://doi.org/10.1021/acsomega.4c05296.

Publisher's Note Springer Nature remains neutral with regard to jurisdictional claims in published maps and institutional affiliations.